A Non-coherent UWB Receiver Using Signal Cluster Sparsity

Sanjeev Sharma[1], Vimal Bhatia[1] (Senior Member, IEEE) and Anubha Gupta[2] (Senior Member, IEEE)
[1] SaSg, Discipline of Electrical Engineering, Indian Institute of Technology Indore, India 453552 {phd1501102011,vbhatia}@iiti.ac.in
[2] SBILab, Department of Electronics and Communication Engg., IIIT-Delhi, New Delhi-110020, anubha@iiitd.ac.in

***Abstract*—The ultra-wide band (UWB) technology can be used for low cost and low power applications such as body area networks, IoT based applications, wireless sensor networks and high data rate short range wireless communications. In the UWB literature, non-coherent energy detector (ED) receiver is proposed to reduce receiver implementation complexity by avoiding the complex channel estimation process and relaxing the precise synchronization requirement. However, the ED receiver performance is sensitive to the integration interval, and too large or small value of integration interval degrades the UWB receiver performance. In this paper, we propose a non-coherent UWB receiver by exploiting the cluster-sparsity of the received UWB signal. The proposed receiver structure enhances the signal-to-noise ratio at the receiver output as compared to the ED by barring inter-clusters noise accumulation. The bit error rate (BER) performance of the proposed non-coherent receiver for time-hopping binary pulse position modulation UWB system is analyzed using IEEE 802.15.4a channel. The proposed receiver design does not require any training and optimization process, and provides 1-3 dB BER performance gain as compared to the conventional ED receiver.**

I. Introduction

The ultra-wide band (UWB) is a low power and low cost technology that has potential applications in wireless sensor network (WSN), body area networks (BAN), internet of things (IoT) based applications, high-accuracy localization, and high data rate wireless local and personal area networks [1–7]. In WSN and IoT based applications, transceivers should be designed with low power consumption and less circuit complexity. Currently, researchers are exploring UWB in IoT based applications using simple system implementation. Also, UWB communication can be used to connect various air interfaces at the physical layer in 5G communication and high data rate (up to 100x gigabits per second) wireless local area networks at millimeter wave communications due to the availability of wide spectrum at high frequencies (above 28 GHz) [8, 9].

In the UWB literature, both coherent and non-coherent receivers are proposed. The performance of coherent receivers is better than the non-coherent receiver. However, coherent receivers have higher system complexity. Coherent receivers such as matched or correlation based UWB receivers are complex and also require high sampling rates [10]. Therefore, these receivers are not suitable for low cost and low power future applications such as WSN and IoT [11]. Another type of receiver proposed in the literature for low data rate communications is transmitted-reference (TR) non-coherent receiver [10, 12]. TR receiver does not have complex channel estimation process. However, TR receiver requires long analog delay line to store the reference signal that is not practical with the current technology.

Non-coherent energy detector (ED) UWB receiver is also proposed in the literature using simple hardware circuitry without the need for channel estimation [6, 10, 12–14]. However, these receivers degrade system performance especially in low signal-to-noise ratio (SNR) regime. Various types of energy detector such as weighted energy detectors (WED) have also been proposed [14–16]. In [17], adaptive weighted ED non-coherent receiver for UWB system is analyzed. This method has significantly increased receiver complexity with marginal improvement in bit error rate (BER) performance (around 0.4 dB only as compared to the conventional ED). In [18], a modified ED receiver for UWB communication is proposed. The receiver design in [18] provides better BER performance compared to the conventional ED. However, it needs training phase to select suitable integration interval and requires an optimum threshold value to combine the multiple integration interval energy in the final decision parameter. In [13], integration interval optimization in ED detector is proposed to enhance receiver performance. However, method in [13] needs joint adaptation of the integration interval and optimal threshold that requires some training.

For the ED based receivers, both small and large values of integration time intervals deteriorate the performance of non-coherent ED receiver. Small integration time interval reduces SNR due to desired signal removal, while large integration time interval reduces SNR due to inclusion of excessive noise in the integration interval. The integration interval optimization and WED require apriori channel knowledge or a complicated weight selection procedure that requires parameter estimation and numerical optimization at the receiver, which enhances the implementation complexity of the receiver. Further, the performance of ED with optimized integration interval is also not optimum in UWB communication due to cluster-sparse nature of the received signal.

In general, the transmitted UWB pulse has shorter time duration as compared to multipath channel delays. As a result, received UWB signal is sparse in nature. This received signal sparsity is observed in the form of clusters, also known as cluster sparsity [19–21]. These clusters have random arrival times at the receiver (depending on the channel impulse response (CIR)). Each cluster's energy is also different and has a random distribution. Thus, in UWB communication,

received signal has desired signal plus noise region (clusters) and noise only region (inter-clusters). Hence, performance of a non-coherent UWB receiver can be improved using only the desired signal plus noise region of the received signal in the receiver design.

We propose a non-coherent UWB receiver using cluster-sparsity of the received UWB signal. In the proposed receiver, the total number of clusters and their energy within a frame duration are calculated using an iterative algorithm. Decision parameter is defined as the weighted combination of clusters' energy using the maximum absolute peak value of each cluster as the weight coefficient. The proposed receiver does not require any training phase, optimization process, and partial channel information unlike WED. The BER performance of the proposed receiver is analyzed for time-hopping binary pulse position modulation (TH-BPPM) UWB system and compared to the conventional ED receiver using IEEE 802.15.4a UWB channel standard. An improved BER performance is observed with the proposed receiver as compared to the conventional ED in additive white Gaussian noise (AWGN), multipath, and multiuser environment.

Rest of the paper is organized as follows: In Section II, basic UWB system using TH-BPPM and ED receiver are described. The proposed receiver design is discussed in Section III. Simulation and discussion are presented in Section IV. Conclusions are drawn in Section V.

II. System Model

In this section, basic UWB system model using TH-BPPM and non-coherent ED receiver are described.

In a UWB system, every data symbol is transmitted over N_f consecutive frames using single pulse per frame to limit the transmitted signal power within the Federal Communications Commission (FCC) spectral mask. The combined signal, $w_c(t)$ of N_f consecutive frames using UWB pulse, $w(t)$ of duration T_w is represented as

$$w_c(t) = \sum_{j=0}^{N_f-1} \left(\sqrt{\frac{E_w}{N_f}}\right) w(t - jT_f - c_j T_c),\ t \in \mathbb{R} \qquad (1)$$

where T_f, T_c, and E_w are frame duration, chip duration, and pulse energy, respectively. $\{c_j\}$ is the pseudo random time hopping (TH) code with a time period N_p and cardinality N_h and is used for smoothing the transmitted signal power spectral density (PSD). The k^{th} transmitted data symbol using TH-BPPM UWB signal can be written as

$$s(t) = \sum_{k=0}^{\infty} w_c(t - kT_s - d_k\Delta), \qquad (2)$$

where $d_k \in \{0, 1\}$ is the data symbol in the k^{th} frame and $T_s = N_f T_f$ is the effective data symbol duration. Δ is the pulse shift parameter for $d_k = 1$ and is also called pulse position modulation index.

The received signal $r(t)$ can be expressed as

$$r(t) = h(t) \otimes s(t) + n(t) = \sum_{l=0}^{L-1} \alpha_l s(t - \tau_l) + n(t), \qquad (3)$$

where $\otimes$ is the convolution operator and $h(t)$ is the CIR that has L number of resolved multipaths and expressed as $h(t) = \sum_{l=0}^{L-1} \alpha_l \delta(t - \tau_l)$, where α_l and τ_l are gain and time delay of l^{th} multipath, respectively. $n(t)$ is AWGN of zero mean and σ_n^2 variance. The received signal $r(t)$ in (3) represents the weighted summation of time shifted transmitted signal $s(t)$ and AWGN $n(t)$. Signal $r(t)$ can be sparse in nature for $\tau_l \geq T_w, \forall\ l$. For non-coherent receiver design, we have considered $\Delta = T_f/2 > T_h + T_w$ with no pulse shape distortion during the transmission, where T_h is the rms (root mean square) delay spread of channel $h(t)$. Therefore, first and second halves of a frame have signals corresponding to $d_k = 0$ and $d_k = 1$, respectively. Further in this paper, SNR is calculated as $SNR = E_{hs}/\sigma_n^2$, where $E_{hs} = \int_{-\infty}^{\infty} (h(t) \otimes s(t))^2 dt$ and CIR $h(t)$ is considered quasi-static for a single frame duration.

In a non-coherent ED receiver, received signal energy is calculated in first and second halves of a frame duration separately. Let $E_1 = \int_0^{T_f/2} r_k^2(t)dt$ and $E_2 = \int_{T_f/2}^{T_f} r_k^2(t)dt$ be the received signal energy in first and second halves of the k^{th} frame respectively, where $r_k(t)$ is the received signal in the k^{th} frame. The transmitted data symbol of the k^{th} frame can be detected using the sign of energy difference $E_1 - E_2$ and is expressed as

$$\hat{d}_k = \begin{cases} 0, & \text{if } (E_1 - E_2) \geq 0 \\ 1, & \text{otherwise} \end{cases},$$

where $\hat{d}_k$ is the detected data symbol in the k^{th} frame at the receiver.

III. Proposed Receiver Design

In this section, we describe the proposed non-coherent receiver design for the UWB communication system. The received UWB signal in a frame appears in the form of clusters. These clusters may be separated from each other. The conventional ED is not optimum because it includes the non-signal portion (noise only region) in the integration interval as well. The proposed receiver uses only the signal clusters in the receiver design and hence, it enhances the SNR at the receiver output by barring inter-clusters noise accumulation.

In order to further analyze the proposed receiver structure, we have considered signal representation from its Nyquist rate samples without any loss of information. Thus, the received signal $r(t)$, CIR $h(t)$, UWB pulse $w(t)$, and AWGN $n(t)$ are represented by vectors as $\mathbf{r} = \big[r(0), r(1), ..., r(N-1)\big]^T$, $\mathbf{h} = \big[h(0), h(1), ..., h(N-1)\big]^T$, $\mathbf{w} = \big[w(0), w(1), ..., w(N-1)\big]^T$ and $\mathbf{n} = \big[n(0), n(1), ..., n(N-1)\big]^T$, where N is the total number of samples at Nyquist rate in a fixed time duration and $[\cdot]^T$ represents the transpose of $[\cdot]$.

The proposed receiver processes the first and second halves of the received signal separately in each frame. Let $\mathbf{r}_1 = \mathbf{r}(1 : N/2)$ and $\mathbf{r}_2 = \mathbf{r}(N/2 + 1 : N)$ represent vectors containing the first and second halves of the received signal in the k^{th} frame, respectively, where N is the total number of samples

in signal $\mathbf{r}$. For $d_k = 0$, signals $\mathbf{r}_1$ and $\mathbf{r}_2$ contain desired signal plus noise and only noise component, respectively. The proposed receiver uses both the number of clusters (NOC) and the time duration of each cluster in the data symbol detection process.

The clusters in a frame are determined as follows: The maximum absolute peak value and its time index are calculated from the received signal $\mathbf{r}_1$ and expressed as

$$\left[P^1_{1,max}, I^1_{1,max}\right] = \max(|\mathbf{r}_1|). \quad (4)$$

First cluster's center is located at $I^1_{1,max}$ with a peak value $P^1_{1,max}$ in $\mathbf{r}_1$. To find the next cluster in $\mathbf{r}_1$, samples of received signal $\mathbf{r}_1$ for the cluster duration around the time index $I^1_{1,max}$ are assigned zero values and this modified received signal is used in (4) in place of $\mathbf{r}_1$ to find the next cluster's center and maximum absolute peak value. This process is repeated until the peak value of a cluster decreases below a predefined '*X*' percentage of the first cluster peak $P^1_{1,max}$, expressed as

$$\text{NOC} = \max\left\{ i : |P^i_{1,max}| \geq \left| \frac{X \times P^1_{1,max}}{100} \right| \right\}, \; i = 1, 2, \ldots \quad (5)$$

where $P^1_{1,max}$ and $P^i_{1,max}$ are the maximum absolute peak values of the first and the i^{th} cluster, respectively. This provides the number of clusters from the received signal.

The duration of each cluster is calculated using the pulse width of the transmitted UWB signal. The pulse time width (non-zero duration) of UWB signal is known apriori in the system by knowing the type of transmitted UWB pulse and its frequency range. Each cluster is assumed to have the same time width and equal UWB pulse time width (assuming no pulse shape distortion during transmission and non-overlapping nature of clusters).

Assuming the cluster width to be of M samples around the cluster peak, a cluster can be expressed as:

$$\mathbf{c}^i_1 = \mathbf{r}_1(I^i_{1,max} - M/2 : I^i_{1,max} + M/2), \; i = 1, 2, ..., \text{NOC}. \quad (6)$$

The energy of each cluster is calculated and expressed as $E^i_1 = \sum_{m=1}^{M} (\mathbf{c}^i_1(m))^2$. To find $\mathbf{c}^i_2$ and E^i_2 using the second half signal $\mathbf{r}_2$, same procedure as outlined above in (4), (5), and (6) is used. The procedure of maximum absolute peak value based cluster finding algorithm is also summarized in **Algorithm 1**.

In the proposed receiver, the received signal energy in the first half of k^{th} frame is expressed as

$$E_{1,k} = \sum_{i=1}^{NOC} P^i_{1,max} E^i_{1,max} \quad (7)$$

In (7), $\{P^i_{1,max}\}_{i=1}^{NOC}$ represents the maximum absolute peak values of the clusters. Therefore, $E_{1,k}$ in (7) represents the weighted summation of cluster energies. The energy $E_{1,k}$ has maximum value due to the optimal weights of $\{E^i_{1,max}\}$ (similar to the maximum ratio combining method). Similar to (7), the received signal energy in the second half of k^{th} frame is expressed as

$$E_{2,k} = \sum_{i=1}^{NOC} P^i_{2,max} E^i_{2,max}. \quad (8)$$

The detected transmitted data symbol $\hat{d}_k$ in the k^{th} frame is calculated using the sign of energy difference $E_{1,k} - E_{2,k}$ and is given as

$$\hat{d}_k = \begin{cases} 0, & \text{if } (E_{1,k} - E_{2,k}) \geq 0 \\ 1, & \text{otherwise} \end{cases}.$$

To analyze the bit error probability of the proposed receiver, let $d_k = 0$. $E^i_{1,max}$ in (7) can be written as

$$E^i_{1,max} = \left\| P^i_{1,max} \frac{\mathbf{w}}{\max(|\mathbf{w}|)} \right\|^2,$$

$$E^i_{1,max} = (P^i_{1,max})^2 \underbrace{\left\| \frac{\mathbf{w}}{\max(|\mathbf{w}|)} \right\|^2}_{E_{w,max}}.$$

where $\mathbf{w}$ constitute UWB pulse as explained at the beginning of this section. Therefore, $E_{1,k}$ in (7) can be rewritten as

$$E_{1,k} = E_{w,max} \sum_{i=1}^{NOC} (P^i_{1,max})^3. \quad (9)$$

The mean value of $E_{1,k}$ is expressed as $\mu_{E_{1,k}} = E_{w,max}\mathbb{E}\left(\sum_{i=1}^{NOC}(P^i_{1,max})^3\right)$, where $\mathbb{E}(\cdot)$ is the statistical average of $(\cdot)$. $E_{1,k}$ has variance $\sigma^2_{E_{1,k}}$ and is given in (10) (on next page).

For the second half of a frame duration, each cluster energy can be written as $E^i_{2,max} = E_{2,max}\ \forall i$ because only noise is present and noise has same distribution in each frame. Thus, $E_{2,k}$ in (8) can be written as

$$E_{2,k} = E_{2,max} \sum_{i=1}^{NOC} P^i_{2,max}. \quad (11)$$

Algorithm 1 Maximum absolute peak value based cluster finding algorithm

Initialize: M, $i = 1$, X, $\mathbf{O}_{1\times M}$- zero vector of size $1 \times M$
Input: Received signal $\mathbf{r}_j,\ j = 1, 2$
Output: $P^i_{j,max}$, $E^i_{j,max}$, NOC
$[P^1_{j,max}, I^1_{j,max}] = \max(|\mathbf{r}_j|)$
While: condition in (5) is true
$\mathbf{c}^i_j = \mathbf{r}_j(I^i_{j,max} - M/2 : I^i_{j,max} + M/2)$
$E^i_j = \sum_{m=1}^{M} (\mathbf{c}^i_j(m))^2$
Update $\mathbf{r}_j(I^i_{j,max} - M/2 : I^i_{j,max} + M/2) = \mathbf{r}_j(I^i_{j,max} - M/2 : I^i_{j,max} + M/2)\mathbf{O}_{1\times M}$
NOC $= i$
$i = i + 1$
$[P^i_{j,max}, I^i_{j,max}] = \max(|\mathbf{r}_j|)$
Do

$$\sigma^2_{E_{1,k}} = E^2_{w,max}\left\{\mathbb{E}\left(\sum_{i=1}^{NOC}(P^i_{1,max})^3\right)^2 - \left[\mathbb{E}\left(\sum_{i=1}^{NOC}(P^i_{1,max})^3\right)\right]^2\right\}. \quad (10)$$

The peak values $P^i_{2,max}\ \forall i$ are selected from the absolute values of Gaussian noise $\mathbf{n}$. Therefore, $P^i_{2,max}$ is distributed as $P^i_{2,max} \sim \mathcal{N}\left(\frac{\sigma_n\sqrt{2}}{\sqrt{\pi}}, \sigma_n^2(1-\frac{2}{\pi})\right)$, where $\mathcal{N}(\mu,\sigma^2)$ represents the Gaussian distribution with mean μ and variance σ^2. After some calculation, the distribution of $E_{2,k}$ can be expressed as $E_{2,k} \sim \mathcal{N}\left(\frac{\text{NOC } E_{2,max}\sigma_n\sqrt{2}}{\sqrt{\pi}}, \text{NOC } E^2_{2,max}\sigma_n^2(1-\frac{2}{\pi})\right)$.

Let $E = E_{1,k} - E_{2,k}$ be the energy difference between the first and the second halves of the k^{th} frame. The probability distribution function (pdf) of energy E can be calculated using the convolution of $E_{1,k}$ and $E_{2,k}$'s pdf and is expressed as $f_E(e) = f_{E_{1,k}}(-e_{1,k}) \otimes f_{E_{2,k}}(e_{2,k})$, where $f_{E_{1,k}}(e_{1,k})$ and $f_{E_{2,k}}(e_{2,k})$ are pdfs of $E_{1,k}$ and $E_{2,k}$ respectively. The theoretical analysis of $f_E(e)$ is left for the future work.

The energy and maximum absolute peak value of each cluster are shown in Fig. 1 for the first and second halves of a frame by considering $d_k = 0$. The value of both energy and maximum absolute peak decreases as cluster index increases in the first half of a frame as shown in Fig. 1 (thin lines in black color). Further, we also observe that energy and maximum absolute peak values' gap decreases between the first and second halves of a frame as the cluster index increases. Therefore, finite number of clusters are used in the detection of k^{th} frame's decision parameters $E_{j,k},\ j = 1, 2$.

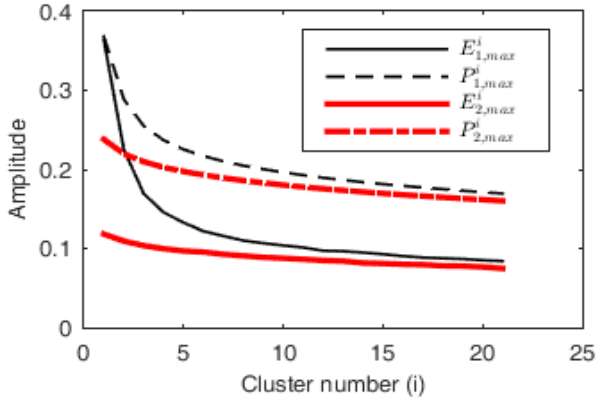

Fig. 1. Cluster energy and peak cluster amplitude for $d_k = 0$ at 20dB SNR.

In Fig. 2, average SNR of each cluster is shown by considering data symbol $d_k = 0$. The SNR of each cluster is calculated using $\frac{E^i_{1,max}-E^i_{2,max}}{E^i_{2,max}}$, where i represents the index of a cluster. The ratio $\frac{E_s-E_n}{E_n}$ represents the SNR of ED receiver in Fig. 2. SNR of individual clusters reduce due to the decreasing value of $E^i_{1,max}$ as the cluster index increases, while $E^i_{2,max}$ remains constant. From Fig. 2, the effective SNR of the proposed receiver is observed to be higher compared to the conventional ED receiver. Further, the number of clusters with higher SNR than the conventional ED receiver can be increased by including $P^i_{j,max}, j = 1, 2$ as the weighting coefficients as shown in Fig. 2 using the blue dashdot line (-·-·-).

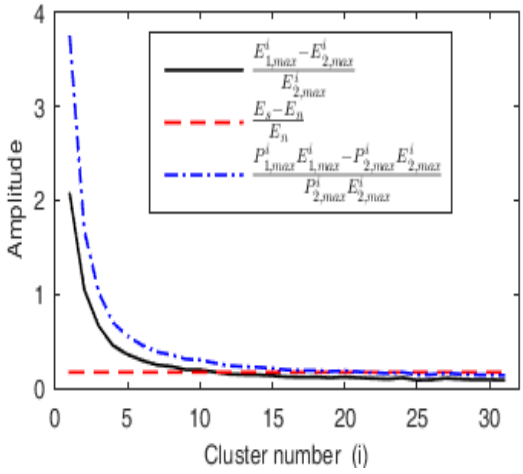

Fig. 2. Average desired signal to noise ratio using the proposed and energy detector receivers for $d_k = 0$ at 20dB SNR.

IV. Simulation and Discussion

In this section, we have carried out simulation using the proposed and ED receivers for the TH-PPM UWB system considered in this work. The transmitted pulse $\mathbf{w}$ is the second derivative of a Gaussian pulse with pulse width parameter $\eta = 0.4$ nanoseconds (ns) and is expressed as given in [22]:

$$w(t) = A\left(1 - \frac{4\pi t^2}{\eta^2}\right)\exp\left(-2\pi t^2/\eta^2\right), \quad t \in \mathbb{R} \quad (12)$$

where A is the pulse amplitude parameter and its value is selected such that pulse $\mathbf{w}$ has unit Euclidean norm. In simulation, 16 GHz is the sampling frequency and data symbol is transmitted using a single frame ($N_f = 1$). The TH code $\{c_j\}$ is generated using $N_h = 3, 7$ and $N_p = 100$ with chip duration $T_c = 1$ ns for AWGN and multipath communication channels, respectively. In simulation results, "CF" and "ED" represent the proposed cluster finding and conventional ED based receivers, respectively.

The average BER performance of TH-BPPM UWB system using the cluster-sparsity based proposed receiver and the ED receiver in AWGN channel is shown in Fig. 3. The BER performance of the proposed receiver is 1-2 dB better than the ED as observed from Fig. 3. This performance improvement using the proposed receiver is due to the reduction in noise accumulation in the decision making parameters $E_{j,k},\ j = 1, 2$ for k^{th} frame.

A. BER performance in multipath channel

Next, we have analyzed the proposed receiver performance in multipath communication scenario using IEEE 802.15.4a channel standard and compared the same with the ED receiver. Multipath channel models CM1, CM2, CM5, and CM8 have been considered in the simulation. More details about these multipath channel models can be found in [23].

The average BER performance of TH-PPM UWB system in line-of-sight (LOS) and non-LOS (NLOS) multipath communication channels in a residential environment using the proposed and the conventional ED receivers is shown in Fig. 4 and Fig. 5, respectively. The proposed receiver provides 1-2 dB better performance in LOS channel CM1 as compared to the ED receiver depending upon the frame duration T_f as observed in Fig. 4. In NLOS channel CM2, BER performance improvement of around 2 dB at BER $= 10^{-4}$ is observed using the proposed receiver as shown in Fig. 5. This performance improvement is observed due to SNR enhancement attributed to the decision making parameters used in the proposed receiver.

The BER performance of the proposed receiver is also analyzed and compared to the ED receiver in LOS channel model CM5 in outdoor UWB communication environment and results are shown in Fig. 6. Using the proposed receiver 1-2 dB gain at BER $= 10^{-4}$ is achieved as compared to the conventional ED as observed in Fig. 6.

Further, the proposed and ED receivers' BER performance is analyzed and compared in NLOS CM9 channel model for farm and snow covered open area communication environment. Results are shown in Fig. 7. Around 3 dB gain at BER $= 10^{-4}$ is achieved using the proposed receiver as compared to the conventional ED as evident from Fig. 7. The performance improvement in CM9 channel model is higher than the other channel models due to higher cluster-sparsity (only few signal clusters) of the received UWB signal.

B. BER performance in multiuser environment

In this subsection, BER performance of TH-PPM UWB system using the proposed receiver is analyzed in multiuser communication environment and is also compared with the ED receiver. In multiuser environment, the received signal is

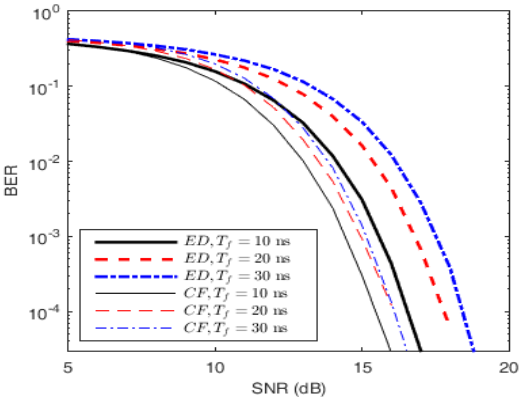

Fig. 3. Average BER vs SNR performance in AWGN channel using the proposed and the ED receivers.

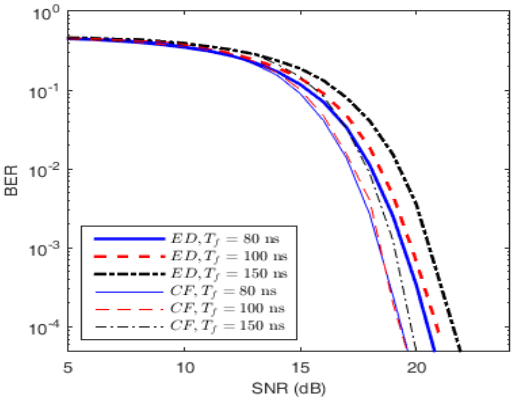

Fig. 4. Average BER vs SNR performance in CM1 multipath communication channel.

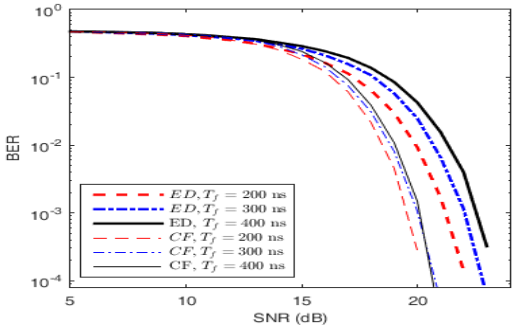

Fig. 5. Average BER vs SNR performance in CM2 multipath communication channel.

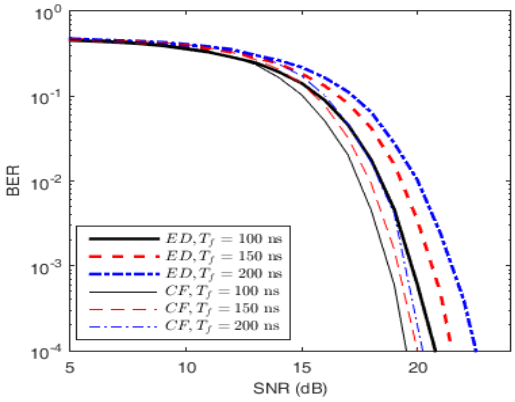

Fig. 6. Average BER vs SNR performance in CM5 multipath communication channel.

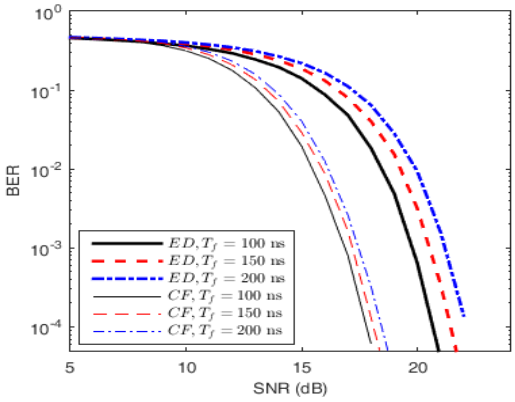

Fig. 7. Average BER vs SNR performance in CM9 multipath communication channel.

expressed as:

$$\mathbf{r} = \underbrace{\mathbf{h} \otimes \mathbf{s}}_{\text{desired user}} + \underbrace{\sum_{u=1}^{U} \mathbf{h}_u \otimes \mathbf{s}_u}_{\text{interference } I_U} + \mathbf{n}, \tag{13}$$

where $\mathbf{h}_u$ and $\mathbf{s}_u$ are the u^{th} interferer's CIR and transmitted signal, respectively. U is the total number of interferes in the system, where each interferer uses the same modulation and transmitted waveform. Without loss of generality, interference I_U is assumed to be of zero mean and $\sigma^2_{I_U}$ variance. The signal-to-interference ratio (SIR) in the multi-users system considered is calculated as $SIR = E_{hs}/\sigma^2_{I_U}$.

The proposed and ED receivers' average BER performance in multiuser interference environment is shown in Fig. 8. The proposed receiver provides 2 dB gain at BER $= 10^{-4}$ and around 2 decades gain at SNR=28 dB for the SIR=8 dB and SIR=5 dB, respectively. Further, the performance of the proposed receiver can be improved using some threshold based cluster energy selection at the decision making stage of the receiver in multiuser communication scenario.

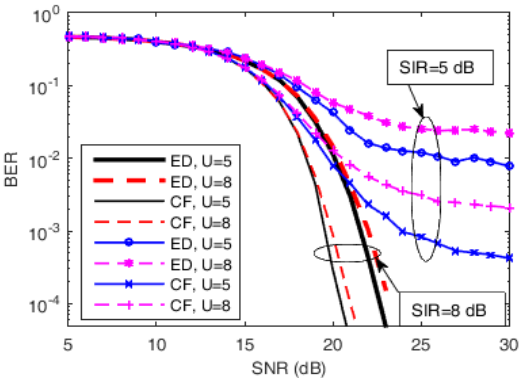

Fig. 8. Average BER vs SNR performance of TH-PPM UWB system in a multiuser communication scenario using the proposed ("CF") and the conventional energy detector ("ED") receivers in CM1 channel model.

Implementation complexity: The proposed receiver design can be implemented in the digital domain with marginal increase in the receiver's implementation complexity. The maximum peak value $P^i_{j,max}$ in each half of a frame has $O(\log(N/2))$ time complexity, where N is the total number of samples in each frame at the Nyquist rate. The value of $E^i_{j,max}$ needs $M-1$ additions and M multiplications, where M is the number of samples in a UWB signal cluster. Further, $E_{j,k}$ computation requires $NOC-1$ and NOC number of additions and multiplications, respectively. Therefore, total number of additions and multiplications required in the proposed receiver design are approximately $NOC\ M$ and $NOC^2\ M$, respectively. The conventional ED requires $N-1$ and N additions and multiplications, respectively. Hence, the total number of multiplications and additions in the proposed receiver are approximately comparable to the ED receiver due to low values of M and NOC (typically in the range of 10-20).

V. Conclusion

In this paper, we have proposed and analyzed a non-coherent receiver by exploiting the cluster based sparsity of the received signal in UWB communication. The proposed receiver is demonstrated to have better BER performance in TH-PPM UWB system compared to the conventional energy detector receiver in AWGN and multipath channels. Better BER performance of the proposed receiver is also associated with a marginal increment in implementation complexity. In the near future, the performance of the proposed receiver will be analyzed for other modulation schemes in UWB communication.

References

[1] A. Bekasiewicz and S. Koziel, "Compact UWB monopole antenna for internet of things applications," *Electronics Letters*, vol. 52, no. 7, pp. 492–494, 2016.

[2] A. Vizziello and P. Savazzi, "Efficient RFID tag identification exploiting hybrid UHF-UWB tags and compressive sensing," *IEEE Sensors Journal*, vol. 16, no. 12, pp. 4932–4939, 2016.

[3] K. Witrisal, S. Hinteregger, J. Kulmer, E. Leitinger, and P. Meissner, "High-accuracy positioning for indoor applications: RFID, UWB, 5G, and beyond," in *IEEE International Conference on RFID*, 2016, pp. 1–7.

[4] H. W. Pflug, J. Romme, K. Philips, and H. de Groot, "Method to estimate impulse-radio ultra-wideband peak power," *IEEE Transactions on Microwave Theory and Techniques*, vol. 59, no. 4, pp. 1174–1186, 2011.

[5] S. Gezici and H. V. Poor, "Position estimation via ultra-wide-band signals," *Proceedings IEEE*, vol. 97, no. 2, pp. 386–403, 2009.

[6] S. Nagaraj and F. Rassam, "Improved non-coherent UWB receiver for implantable biomedical devices," *IEEE Transactions on Biomedical Engineering*, vol. 63, no. 10, 2016.

[7] S. Sharma, A. Gupta, and V. Bhatia, "A new sparse signal-matched measurement matrix for compressive sensing in UWB communication," *IEEE Access*, vol. 4, pp. 5327–5342, 2016.

[8] S. Harrison and P. F. Driessen, "Novel UWB and spread spectrum system using time compression and overlap-add techniques," *IEEE Access*, vol. 2, pp. 1092–1105, 2014.

[9] N. Rendevski and D. Cassioli, "60 GHz UWB rake receivers in a realistic scenario for wireless home entertainment," in *IEEE International Conference on Communications (ICC)*, 2015, pp. 2744–2749.

[10] K. Witrisal, G. Leus, G. J. Janssen, M. Pausini, F. Trösch, T. Zasowski, and J. Romme, "Noncoherent ultra-wideband systems," *IEEE Signal Processing Magazine*, vol. 26, no. 4, pp. 48–66, 2009.

[11] K. Allidina, T. Khattab, and M. N. El-Gamal, "On dual peak detection UWB receivers in noise and interference dominated environments," *AEU-International Journal of Electronics and Communications*, vol. 70, no. 2, pp. 121–131, 2016.

[12] A. Rabbachin, T. Q. Quek, P. C. Pinto, I. Oppermann, and M. Z. Win, "Non-coherent UWB communication in the presence of multiple narrowband interferers," *IEEE Transactions on Wireless Communications*, vol. 9, no. 11, pp. 3365–3379, 2010.

[13] M. E. Sahin, I. Guvenc, and H. Arslan, "Optimization of energy detector receivers for UWB systems," in *IEEE 61st Vehicular Technology Conference (VTC)*, vol. 2, 2005, pp. 1386–1390.

[14] A. Gerosa, S. Soldà, A. Bevilacqua, D. Vogrig, and A. Neviani, "An energy-detector for noncoherent impulse-radio UWB receivers," *IEEE Transactions on Circuits and Systems I: Regular Papers*, vol. 56, no. 5, pp. 1030–1040, 2009.

[15] X. Cheng, Y. L. Guan, and S. Li, "Optimal BER-balanced combining for weighted energy detection of UWB OOK signals," *IEEE Communications Letters*, vol. 17, no. 2, pp. 353–356, 2013.

[16] F. Wang, Z. Tian, and B. M. Sadler, "Weighted energy detection for noncoherent ultra-wideband receiver design," *IEEE Transactions on Wireless Communications*, vol. 10, no. 2, pp. 710–720, 2011.

[17] Z. Liang, P. Li, J. Zang, J. Liu, and X. Peng, "Adaptive weighted energy detection receivers for NC-PPM-UWB communication systems," in *IEEE 9th International Conference on Signal Processing and Communication Systems (ICSPCS)*, 2015, pp. 1–5.

[18] N. Decarli, A. Giorgetti, D. Dardari, M. Chiani, and M. Z. Win, "Stop-and-go receivers for non-coherent impulse communications," *IEEE*

Transactions on Wireless Communications, vol. 13, no. 9, pp. 4821–4835, 2014.

[19] X. Sun, Y. Jia, M. Hou, and C. Zhao, "60 GHz ultra-wideband channel estimation based on a cluster sparsity compressed sensing," *EURASIP Journal on Wireless Communications and Networking*, vol. 2013, no. 1, pp. 1–9, 2013.

[20] J. L. Paredes, G. R. Arce, and Z. Wang, "Ultra-wideband compressed sensing: channel estimation," *IEEE Journal of Selected Topics in Signal Processing*, vol. 1, no. 3, pp. 383–395, 2007.

[21] X. Cheng, M. Wang, and Y. L. Guan, "Ultrawideband channel estimation: A bayesian compressive sensing strategy based on statistical sparsity," *IEEE Transactions on Vehicular Technology*, vol. 64, no. 5, pp. 1819–1832, 2015.

[22] S. Sharma, V. Bhatia, and A. Gupta, "Sparsity based UWB receiver design in additive impulse noise channels," in *IEEE 17th International Workshop on Signal Processing Advances in Wireless Communications (SPAWC)*, 2016, pp. 1–5.

[23] A. F. Molisch, D. Cassioli, C.-C. Chong, S. Emami, A. Fort, B. Kannan, J. Karedal, J. Kunisch, H. G. Schantz, K. Siwiak *et al.*, "A comprehensive standardized model for ultrawideband propagation channels," *IEEE Transactions on Antennas and Propagation*, vol. 54, no. 11, pp. 3151–3166, 2006.